Case Studies in Construction Materials 22 (2025) e04563

Contents lists available at ScienceDirect

Case Studies in Construction Materials

journal homepage: www.elsevier.com/locate/cscm

Case study

Influence of ammonia-contaminated fly ash from selective catalytic reduction process on the properties of Portland-fly ash blended cement and geopolymer composites

Teewara Suwan [a,b,*], Mizi Fan [c], Hong S. Wong [d], Peerapong Jitsangiam [b,e], Chayanon Hansapinyo [a], Prinya Chindaprasirt [f]

[a] *Excellence Center in Infrastructure Technology and Transportation Engineering, Department of Civil Engineering, Chiang Mai University, Chiang Mai 50200, Thailand*
[b] *Chiang Mai University Advanced Railway Civil and Foundation Engineering Center, Department of Civil Engineering, Faculty of Engineering, Chiang Mai University, Chiang Mai 50200, Thailand*
[c] *Department of Civil and Environmental Engineering, College of Engineering, Design and Physical Sciences, Brunel University, Uxbridge, London UB8 3PH, UK*
[d] *Centre for Infrastructure Materials, Department of Civil and Environmental Engineering, Imperial College London, London SW7 2AZ, UK*
[e] *Multidisciplinary Research Institute, Chiang Mai University, Chiang Mai 50200, Thailand*
[f] *Sustainable Infrastructure Research and Development Center, Department of Civil Engineering, Faculty of Engineering, Khon Kaen University, Khon Kaen 40002, Thailand*

ARTICLE INFO

Keywords:
Ammonia-contaminated fly ash
Selective catalytic reduction
Supplementary cementitious materials
Compressive strength
Pozzolanic activity
Sustainable construction

ABSTRACT

Fly ash, a by-product of coal-fired power plants, finds valuable application in the cement and concrete industry due to its pozzolanic properties. Environmental concerns necessitate the use of Selective Catalytic Reduction (SCR) systems to reduce nitrogen oxide emissions; however, this process introduces residual ammonia onto the fly ash, known as SCR-fly ash, which may affect its properties. This study investigates the characteristics and suitability of SCR-fly ash as a supplementary cementitious material in Portland cement and geopolymer cement composites, compared to conventional high-calcium fly ash. The results show that Portland-fly ash blended cement mixtures containing 20 % SCR-fly ash achieve comparable engineering properties to those with high-calcium fly ash, with a slight reduction in compressive strength of ~ 3.4 % at 28 days. Geopolymers with SCR-fly ash exhibit a significantly lower (~ 52.8 %) compressive strength than that of high-calcium fly ash 28 days. However, SCR-fly ash requires a resting period of at least 20 days to reduce ammonia content before use. The larger particle size and presence of residual ammonia can react to form detrimental gypsum or ammonium salts that lead to reduced strength. Therefore, SCR-fly ash may need to be chemically treated to be suitable as a geopolymer precursor. Overall, this work provides crucial insights into the potential utilization of SCR-fly ash in the cement and concrete industry, promoting resource recovery and environmental sustainability.

---

* Corresponding author at: Excellence Center in Infrastructure Technology and Transportation Engineering, Department of Civil Engineering, Chiang Mai University, Chiang Mai 50200, Thailand.
E-mail address: teewara.s@cmu.ac.th (T. Suwan).

https://doi.org/10.1016/j.cscm.2025.e04563
Received 29 December 2024; Received in revised form 13 March 2025; Accepted 19 March 2025

1. Introduction

Fly ash, a byproduct of coal-fired power plants, is widely utilized in the cement and concrete industry due to its pozzolanic properties, which enhance strength, durability, and sustainability in construction. Traditionally, fly ash has been sourced from electrostatic precipitators, but recent environmental regulations aimed at reducing nitrogen oxide (NOx) emissions have led to the adoption of Selective Catalytic Reduction (SCR) systems. While these systems effectively mitigate air pollution, they introduce residual ammonia contamination in fly ash, potentially altering its physical, chemical, and mechanical properties. This ammonia-contaminated fly ash, referred to as SCR-fly ash, poses challenges and opportunities for its use as a supplementary cementitious material. Understanding the implications of ammonia contamination is crucial, as it may influence hydration kinetics, setting behaviour, and long-term performance in both Portland cement and geopolymer cement applications. As SCR technology becomes widespread, further research is needed to evaluate SCR-fly ash's feasibility in sustainable construction while mitigating durability concerns.

1.1. Fly ash in Portland cement and geopolymer cement

Fly ash is a major industrial by-product of coal-fired power stations. In the past, fly ash was considered a low-value waste and was often discarded in landfill sites. This resulted in various environmental problems, including the contamination of soil and water resources by leached heavy metals and harmful substances, and the release of micro-fly ash particles into the local atmosphere. As such, many attempts have been made to mitigate these problems over the past decades and a successful practical approach is to valorise fly ash in the cement and concrete industry [1,2].

Fly ash is commonly used as supplementary cementitious material (SCM) to partially replace Portland cement (OPC) for concrete production. Its chemical and physical properties are specified in standards, for example the ASTM C618 [3]. The use of fly ash reduces the OPC content in concrete, and therefore its overall cost and embodied carbon. Moreover, the spherical shape of fly ash can significantly enhance flowability and workability of the fresh concrete [4]. The pozzolanic reaction of fly ash leads to the formation of additional calcium silicate hydrate (C-S-H) that improves long-term strength and durability of the concrete. In addition, fly ash has been used to produce alternative cementitious materials, such as alkaline activated “geopolymer” cements [5].

Geopolymer cement (GP) is an alternative to OPC that reuses industrial wastes for low-carbon concrete production. GP is typically synthesized using pozzolanic aluminosilicate precursors such as fly ash, bottom ash, metallurgical slags and calcined clays [6]. Alkaline activators such as sodium hydroxide or sodium silicate are used to activate the polymeric reactions that form C-S-H and calcium/sodium aluminosilicate hydrate (C-A-S-H/N-A-S-H) phases. In most cases, heat curing at around 40–90 °C for 6–24 h is applied to accelerate the reaction and achieve better engineering performance [5,7]. Since GP can be synthesized from waste precursors without requiring OPC, it offers many environmental and practical advantages.

However, the properties of fly ash depend on many factors such as the type of coal, installed system, preparation and combustion process, hazardous gases removal, fly ash collection, storage and others [8]. As such, fly ash is a heterogeneous waste material and the variability in its properties has significant implications on its utilization potential.

1.2. Fly ash from SCR process

Combustion activities produce NO_x emissions that are harmful to human and animal health. There are two NO_x reduction processes currently in use, selective non-catalytic reduction (SNCR) and selective catalytic reduction (SCR). Both are based on the injection of ammonium compounds into the combustion chamber. However, SNCR consumes much higher energy to reach the required operating temperature than the catalytic-based SCR process [8–10]. Therefore, SCR is more widespread and has undergone significant developments in many industries over the past decades. Furthermore, SCR is capable of capturing other pollutants such as SO_x and small particulate matter that are relevant to coal-fired power stations [11,12].

The core principle behind the SCR system is the injection of aqueous ammonia or urea and other reductants into the furnace or flue gas combustion chamber to convert NO_x to N_2 and water according to Eq. (1).

$$NO + NO_2 + 2NH_3 \rightarrow 2N_2 + 3H_2O \tag{1}$$

Although this is highly effective for removing NO_x, it has been found that some unreacted ammonia can escape from the chamber during the injection process and contaminate the collected fly ash [9]. As a result, the properties of fly ash from the SCR process, so-called ‘*SCR-fly ash*’, are different from that of typical fly ash. This issue has become a major concern for the cement and concrete industry that wishes to utilize SCR-fly ash as an SCM [9,11]. However, the effects of contaminated SCR-fly ash on the properties of fresh and hardened concrete are not well established [9].

1.3. Challenges and opportunities for utilizing SCR-fly ash in concrete

Globally, there is a growing demand for low-carbon cement and concrete materials to satisfy infrastructure development in a sustainable manner. However, there is a dwindling limited supply of conventional fly ash, and the typical fly ash precipitator is increasingly being replaced by the SCR process. SCR-fly ash is thus becoming an attractive option for the concrete industry [13,14]. Previous studies on SCR-fly ash found that a limited amount of ammonia contamination can be controlled by adjusting the catalysts or chamber temperature [15,16], leading to additional operating costs. Michalik et al. [9] showed that direct use of SCR-fly ash in

OPC-based concrete decreased mechanical strength compared to typical fly ash blended concrete due to an unexpected expansion caused by ammonia. As such, a resting time to allow for the release of ammonia from SCR-fly ash before use has been recommended [17,18].

As a case study, the largest coal-fired power plant in Thailand (Mae Moh power plant) is now transitioning from an ultra-supercritical process with low NO_x burner to the SCR process for fly ash collection and storage. With the environmental policies mandated by the Electricity Generating Authority of Thailand (EGAT), this 2200-Megawatt Mae Moh power plant will be required to utilize their massive amount of generated SCR-fly ash very soon. A study on the possible utilization of SCR-fly ash in the concrete industry is therefore urgently required. Given the concerns about the presence of ammonia posing a risk to long-term performance [9, 19], this study aims to investigate the effects of SCR-fly ash on the fresh and hardened state properties of Portland blended cement and geopolymer cement-based materials.

While the use of fly ash as a supplementary cementitious material is well established, the influence of SCR-fly ash on cementitious systems remains inadequately studied. Previous research has primarily focused on conventional high-calcium fly ash, with limited insight into how residual ammonia affects hydration reactions, setting time, and long-term mechanical performance. Additionally, the potential risks associated with ammonium-based reaction by-products have not been thoroughly quantified. This study addresses these gaps by systematically evaluating the engineering properties, microstructural characteristics, and chemical interactions of SCR-fly ash in both OPC-fly ash blended cement and geopolymer systems. The results will offer valuable insights for incorporating SCR-fly ash into sustainable construction methods while addressing potential durability challenges.

2. Experimental program

2.1. Materials

Portland Cement (OPC) Type 1 ASTM C150 with a specific gravity of 3.14 was used. Two types of fly ashes from Mae Moh coal-fired power plant (Lampang province, Thailand) were used. These were typical high calcium fly ash (HC-fly ash) and fly ash from the selective catalytic reduction process (SCR-fly ash). These had a specific gravity of 2.85 and 2.58, respectively. Table 1 shows the main oxide compositions of OPC, HC-fly ash and SCR-fly ash from X-ray fluorescence (XRF) analysis. The SCR-fly ash was collected from the power plant and stored in a dry and cool location for approximately 200 days before casting. A mixture of sodium hydroxide and sodium silicate solution was used as an alkali activator for geopolymer samples. Micro-pearl sodium hydroxide (NaOH, 99 % purity) was used to prepare a 10-molar sodium hydroxide solution. The sodium silicate solution (Na_2SiO_3) was SL-2.4 C grade of 45.83 % w/w and silicate modulus (Ms) of 2.10 (16.3 % Na_2O, 34.2 % SiO_2, and 49.5 % H_2O).

2.2. Fly ash characterization

The fly ashes were characterized using various techniques. Scanning electron microscopy (SEM, JEOL JSM-5910LV) was used at 30 kV in vacuum mode to observe microstructure. A Malvern Zetasizer ZS particle size analyzer was used to determine particle size distribution in the range of 0.3 nm to 10.0 microns. X-ray diffraction (XRD) was conducted using a 4-circle kappa goniometer diffractometer with a microfocus sealed tube (Mo) and direct photon-counting detector (HyPix-Bantam), to investigate crystalline composition. Fourier Transform Infrared (FT-IR, Thermo Nicolet 6700) spectroscopy with attenuated total reflectance (ATR) was used to identify functional groups within spectral wavelengths 450–4000 cm^{-1}. A potassium chloride (KCl) extraction technique was specifically adapted with colorimetry to produce a colored compound for spectrophotometric measurement of ammonium residue concentration in the SCR-fly ash. KCl solution was used to leach ammonium ions from the fly ash particles, preventing the conversion of ammonium ions (NH^{4+}) to ammonia gas (NH_3) in alkaline environments. The concentration of ammonium residue in the SCR-fly ash was determined after 10, 20, 30, and 200 days of storage following collection from the power plant.

2.3. Mix proportions

A total of nine cement paste mixes were prepared. These were divided into two series: I) OPC-fly ash blended cement mixes, and II) geopolymer cement mixes. Details of mixture proportions are presented in Table 2.

The OPC-fly ash blended cement mixtures were prepared at a water-to-cement (w/c) ratio of 0.35. The OPC-to-fly ash mass ratio was varied from 100:0 (control mix) to 80:20, 60:40, and 40:60. Wet mixing was carried out for 90 s at 140 ± 5 rpm at a room temperature of 28 ± 2 °C. After thorough mixing, the fresh cement paste was cast into 40 × 40 × 160 mm prism moulds (EN 196-1) and wrapped immediately with plastic sheeting to prevent moisture loss. Then, the samples were demoulded, wrapped with plastic sheeting again, and sealed cured at room temperature (28 ± 2°C) until reaching the testing age of 3, 28, and 90 days.

Table 1
Chemical compositions (oxides) of the binders from XRF analysis (%).

Material	SiO_2	Al_2O_3	Fe_2O_3	CaO	SO_3	SrO	MnO	K_2O	LOI
OPC	11.93	2.46	4.06	74.96	4.89	-	-	1.03	1.0
HC-fly ash	17.99	8.61	30.31	31.73	7.71	0.29	0.22	2.55	N/A
SCR-fly ash	22.75	10.67	27.17	29.23	6.09	0.26	0.23	2.72	N/A

Table 2
Mix proportions for OPC-fly ash blended cement and geopolymer cement pastes.

Series	Mix ID	w/c ratio	L/B ratio	OPC (%)	HC-FA (%)	SCR-FA (%)
I) OPC-fly ash blended cement	Control OPC	0.35	-	100	-	-
	HC-FA20	0.35	-	80	20	-
	HC-FA40	0.35	-	60	40	-
	HC-FA60	0.35	-	40	60	-
	SCR-FA20	0.35	-	80	-	20
	SCR-FA40	0.35	-	60	-	40
	SCR-FA60	0.35	-	40	-	60
II) Geopolymer	HC-FA GP	-	0.60	-	100	-
	SCR-FA GP	-	0.60	-	-	100

The geopolymer cement mixtures were prepared using a 1:1 mixture of 10 molar sodium hydroxide solution and sodium silicate solution as the alkaline activator. The prepared alkaline solution was added to fly ash at a liquid-to-binder (L/B) mass ratio of 0.60 to achieve good workability. Wet mixing was carried out for 90 s at 140 ± 5 rpm at a room temperature of 28 ± 2 °C in a 5-l mortar mixer. After thorough mixing, the fresh geopolymer mixture was cast into prismatic moulds and wrapped immediately with plastic sheeting to prevent moisture loss. The samples were demoulded after 24 h, then wrapped with plastic sheeting and sealed cured at room temperature until reaching the testing age of 3, 28, and 90 days.

2.4. *Tests*

The prepared paste samples were subjected to fresh and hardened state properties testing. Fresh cement pastes were tested for setting time using a Vicat apparatus according to ASTM C191 and flowability using a flow table apparatus according to ASTM C1437. Compressive strength was measured using 40 mm × 40 mm × 40 mm cubic specimens cut from the prepared prisms. For each mix, six specimens were tested in accordance with the EN 196-1 standard using a 250 kN Controls universal testing machine. Additionally, scanning electron microscopy (SEM), X-ray diffraction (XRD), and Fourier Transform Infrared (FT-IR) analysis were conducted to investigate the phase assemblage and microstructural changes within the samples.

3. Results and discussion

3.1. *Fly ash characterization*

3.1.1. *Particle size distribution*

Figs. 1 and 2 show the average particle size distribution from two replicate batches of the fly ashes, as determined using the Malvern particle size analyzer. The average D10, D50, and D90 of SCR-fly ash were 4.7 μm, 20.7 μm, and 113.0 μm, respectively. In contrast, the corresponding values for HC-fly ash were 2.9 μm, 10.6 μm, and 32.0 μm, respectively. HC-fly ash exhibited a smaller volumetric mean diameter (14.5 μm) and a correspondingly higher specific surface area (0.879 m^2/g) compared to SCR-fly ash (39.1 μm and 0.516 m^2/g, respectively). The specific surface area of SCR-fly ash exhibited variability, likely due to its origin from a different power plant compared to the HC-fly ash. It is worth noting that the differences in the particle size distribution of SCR-fly ash can be attributed to variations in its production processes and physicochemical properties. Residual ammonia in SCR-fly ash can promote particle agglomeration, resulting in a broader, coarser, and less uniform particle distribution. Additionally, these differences also depend on variations in combustion temperatures, coal types, and SCR system configurations [20].

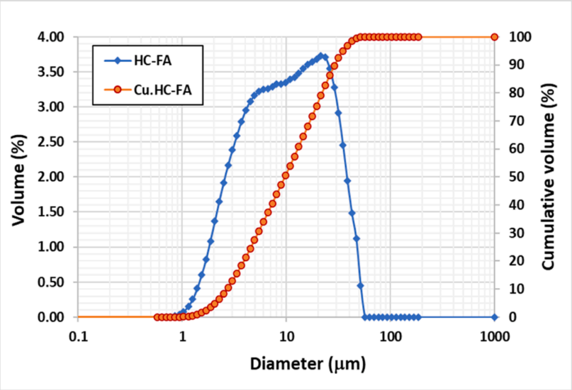

Fig. 1. Particle size distribution of HC-fly ash.

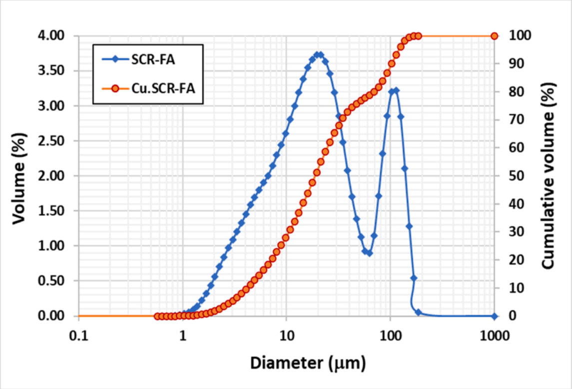

Fig. 2. Particle size distribution of SCR-fly ash.

These observations were corroborated by SEM at 500 × magnification (Fig. 3), which revealed a predominantly spherical morphology for both fly ashes due to the electrostatic collection process. The SEM images qualitatively confirmed the significantly smaller size of HC-fly ash compared to SCR-fly ash. The difference in FA particle size could influence reaction rates when blended in a Portland cement or geopolymer cement system.

3.1.2. *Ammonia content*

Previous studies on denitrification through SCR and SNCR under similar conditions were conducted by Michalik et al. and Larrimore [9,11]. Therefore, some of their findings were used as comparison in assessing the reduction of ammonia concentration in Mae Moh SCR-fly ash over the observed time period of 0–200 days after collection. The highest reduction (roughly 50 %) occurred within the first 20 days of exposure to ambient air for samples No. 1–4 [9,10]. Literature suggests that the excess ammonia content in fly ash can range from 50 to 300 mg/kg [9,11]. While previous studies reported significantly higher ammonia levels in SCR-fly ash [10,11], all observed a similar trend of decreasing ammonia content over time, especially within the first few weeks.

Fig. 4 shows the ammonia content in fly ash measured from the literature and from the KCl extraction method for Mae Moh SCR-fly ash samples after storage periods of 10, 20, 30, and 200 days. The ammonia content in SCR-fly ash from the Mae Moh power plant decreased from 12.4 mg/kg to 2.2 mg/kg. Importantly, no ammonia was detected in the HC-fly ash samples. It can be observed that ~ 50 % of ammonia reduction occurs within the first 20 days of exposure to ambient air, similar to previous studies [9–11]. It is worth noting that the cement mixtures in the current study were prepared with 200-day-old Mae Moh SCR-fly ash.

3.1.3. *Functional groups and amorphous phases*

Fig. 5 shows the FT-IR spectra of HC-fly ash and SCR-fly ash within the first few days after collection. Strong bands corresponding to Si-O-Si and Al-O stretching vibrations were observed around 465–500 cm^{-1}, 620–700 cm^{-1}, and 790–800 cm^{-1}, indicating the abundance of silicon and aluminium in the samples. A broad peak around 1630–1700 cm^{-1} is attributed to O-H bending in adsorbed water. A unique broad peak around 1400–1450 cm^{-1} was identified, potentially indicating either C-H bending in residual organic matter or the presence of carbonate (CO_3) groups. Since SCR-fly ash used ammonia (NH_3) for NOx capture, N-H bending vibrations in ammonium

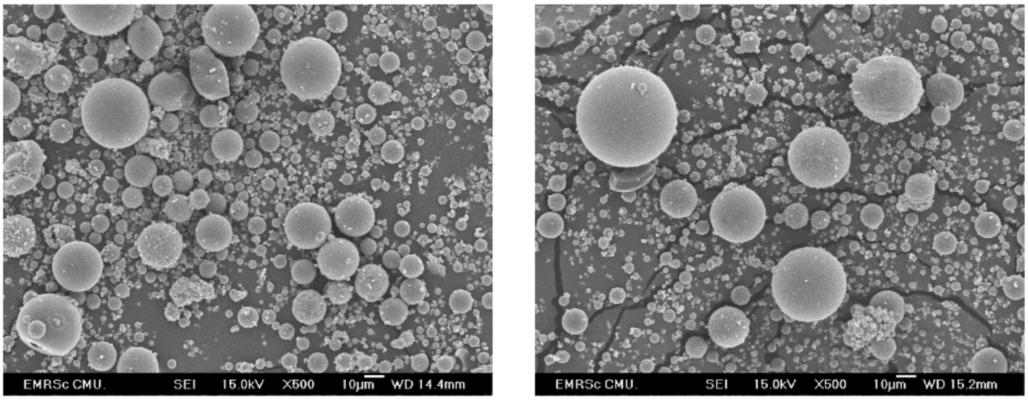

a) HC-fly ash b) SCR-fly ash

Fig. 3. SEM images of HC-fly ash, and SCR-fly ash at 500x magnification.

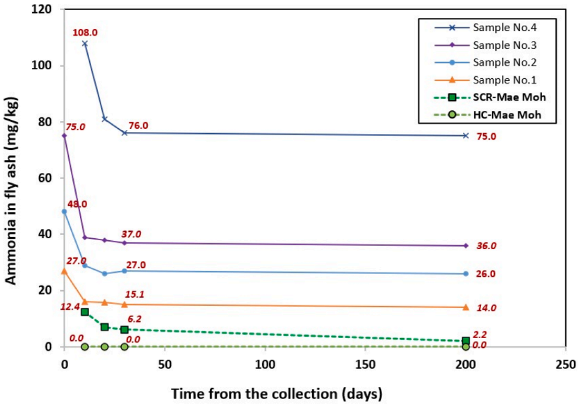

Fig. 4. Ammonia in Mae Moh SCR-fly ash and HC-fly ash after different storage durations following collection from the power plant.

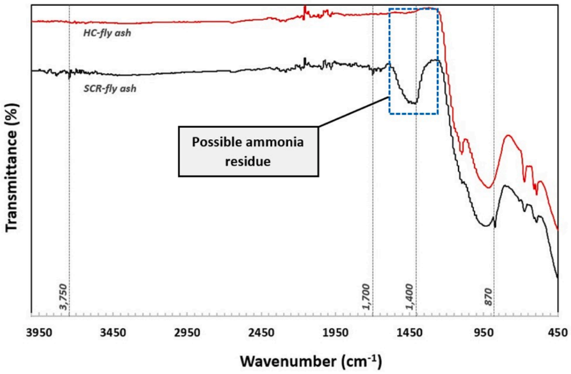

Fig. 5. FT-IR spectra of HC-fly ash and SCR-fly ash.

salts or ammonium ions (NH_4^+), typically appearing around 1400–1390 cm^{-1}, can be detected, occasionally overlapping with other functional groups.

XRD analysis revealed no significant compositional differences between the HC-fly ash and SCR-fly ash samples (see Fig. 6). Typical phases were identified by their characteristic peaks including quartz (Q; SiO_2), mullite (M; $3Al_2O_3$–$2SiO_2$), and magnetite (Mt; Fe_3O_4). Additionally, hematite (Ht; Fe_2O_3), hercynite (H; $FeAl_2O_4$), and periclase (P; MgO) were detected, further confirming the expected compositional profile of the fly ash. Broad humps observed between 10° and 40° 2θ in the patterns of both fly ashes indicate the presence of amorphous phases.

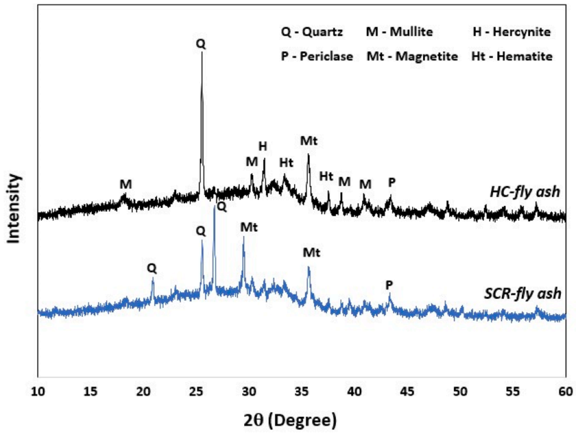

Fig. 6. X-ray diffraction patterns of HC-fly ash and SCR-fly ash.

Quantitative analysis using the embedded Match! program, performed by calculating the area under the respective XRD patterns, revealed an amorphous phase content of 61.2 % and 38.8 % crystalline phase content for HC-fly ash, and 59.9 % amorphous and 40.1 % crystalline phase content for SCR-fly ash. These results show that there are no significant differences in the overall phase compositions of the fly ash samples.

3.2. *Setting time, flowability and unit weight*

Fig. 7a presents the initial and final setting times of the cement pastes. The pure OPC paste was used as a control reference which exhibited initial and final setting times of 114 min and 240 min, respectively. The pastes containing SCR- or HC-fly ash demonstrated longer setting times compared to the control, attributable to the retardation effect of fly ash on early-age reactions. The setting time increased proportionally with the amount of fly ash, with the SCR-fly ash mixtures exhibiting a longer delay compared to HC-fly ash mixtures. This difference is probably due to the larger particle sizes of SCR-fly ash. Consequently, the setting behaviour of SCR-fly ash blended cement is more delayed compared to that of HC-fly ash blended cement.

The geopolymer mixtures exhibited a flash setting behaviour, particularly for the HC-fly ash geopolymer, which had an initial setting time of only 5–10 min. In contrast, the SCR-fly ash geopolymer had a slightly longer initial setting time of 50–60 minutes. Both fly ashes, classified as high calcium Class C fly ash (ASTM C618), typically exhibit rapid reactions when combined with a strong alkaline solution (NaOH activator) [7]. Despite their similar chemical compositions, as determined by XRF analysis, differences in particle size and SiO_2/Al_2O_3 ratios probably influenced their setting times. SCR-fly ash has larger particle sizes and a slightly higher

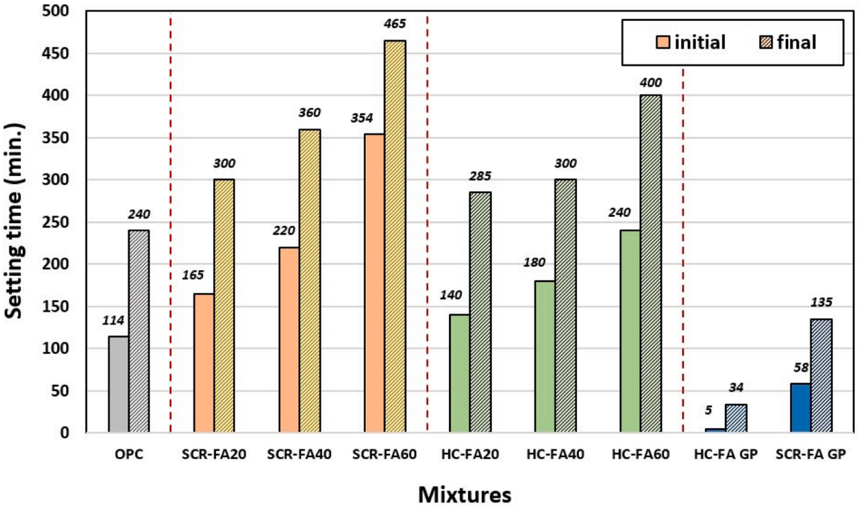

a Setting time.

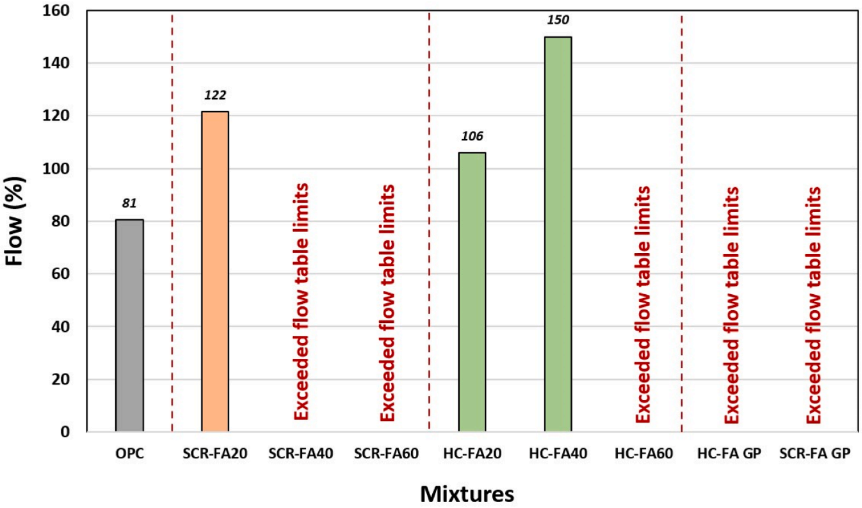

b Flowability.

Fig. 7. Setting time and workability of OPC-fly ash blended cement and geopolymer cement pastes.

SiO_2/Al_2O_3 ratio (2.14) compared to HC-fly ash (2.08). A higher SiO_2/Al_2O_3 ratio can result in a longer setting time due to the slower dissolution rate of SiO_2. Conversely, a lower ratio leads to rapid setting time but can compromise mechanical integrity of the geopolymer due to insufficient silicate species necessary for network formation [21,22].

Fig. 7b shows the workability of the pastes, assessed using the flow table test. The OPC mix exhibited a flowability of 81 % (of the test plate diameter), while both 20 % fly ash replacement mixtures (SCR-FA20 and HC-FA20) demonstrated higher flowabilities at 122 % and 106 %, respectively. The smaller particle size and higher surface area of HC-fly ash increased water demand and reaction compared to SCR-fly ash, resulting in a decreased spread (lower fluidity) in the flow table test. Mixtures with over 40 % fly ash replacement exceeded the flow table limits, meaning they were too fluid to measure accurately. It was observed that excessive fly ash content led to flow values that exceeded the dimension of the flow table test (Fig. 7b). This indicates that while moderate fly ash replacement can enhance workability, too high a replacement level can result in excessive fluidity, complicating the measurement and potentially affecting the structural integrity of the cement [23].

Fig. 8 shows the unit weight of the cement pastes at 28 days of age. The OPC reference paste had a unit weight of 1.978 g/cm^3. For OPC-fly ash blended pastes, both SCR- and HC-fly ash replacements (at 20 %, 40 %, and 60 %) led to a gradual decrease in the unit weight of the samples initially. However, after hydration and pozzolanic reaction over time, HC-fly ash blended pastes achieved a slightly higher unit weight and therefore a denser microstructure. A factor contributing to this could be the smaller, spherical particles of HC-fly ash compared to SCR-fly ash. A similar trend was observed in the geopolymer pastes, where HC-fly ash-based geopolymer achieved a higher unit weight of 2.023 g/cm^3 compared to 1.935 g/cm^3 for SCR-fly ash-based geopolymer.

3.3. Compressive strength

Fig. 9 shows the compressive strength of the cement pastes at 3, 28, and 90 days of age. The results indicate variations in the compressive strength across different mixtures, age and replacement levels of fly ash. The OPC reference mixture exhibited a compressive strength of 50.7 MPa at 3 days, 56.1 MPa at 28 days, and 72.0 MPa at 90 days. The OPC-fly ash blended paste showed decreasing compressive strength with increasing fly ash content. Specifically, the SCR-fly ash mixtures showed a compressive strength of 40.6 MPa, 53.4 MPa, and 70.6 MPa at 20 % replacement; 27.4 MPa, 50.9 MPa, and 63.3 MPa at 40 % replacement; and 17.2 MPa, 40.5 MPa, and 49.0 MPa at 60 % replacement at 3, 28, and 90 days, respectively. In comparison, the HC-fly ash mixtures demonstrated slightly higher compressive strengths: 42.6 MPa, 55.3 MPa, and 71.4 MPa at 20 % replacement; 29.4 MPa, 51.0 MPa, and 68.0 MPa at 40 % replacement; and 19.5 MPa, 45.6 MPa, and 51.0 MPa at 60 % replacement at 3, 28, and 90 days, respectively. At the standard cement testing age of 28 days, it was found that OPC-fly ash blended mixtures containing 20 % SCR-fly ash (53.4 MPa) achieved comparable average engineering properties to those containing 20 % HC-fly ash (55.3 MPa), with a slight reduction in compressive strength of approximately 3.4 %. And, at the same age and fly ash replacement percentages, SCR-fly ash achieved slightly lower strength than the HC-fly ash mixtures by 0.2 % and 11.2 % for 40 % and 60 % FA replacement, respectively. Nevertheless, the significant increase in strength with age is attributed to the formation of additional secondary calcium silicate hydrate (C-S-H) from the pozzolanic reaction between $Ca(OH)_2$ and fly ash [24].

The results indicate that the type of fly ash has a slight impact on compressive strength development. This may be attributed to differences in particle size, surface area, and the presence of residual ammonia in SCR-fly ash. The presence of ammonia (as ammonium sulfate; $(NH_4)_2SO_4$) has been reported to react with calcium hydroxide ($Ca(OH)_2$), forming unwanted gypsum as shown in Eq. (2) [25]. Therefore, it is important to impose a resting period of approximately 20–30 days (see Fig. 4) after collection to allow for the attenuation of ammonia before utilizing SCR-fly ash as an SCM in concrete production.

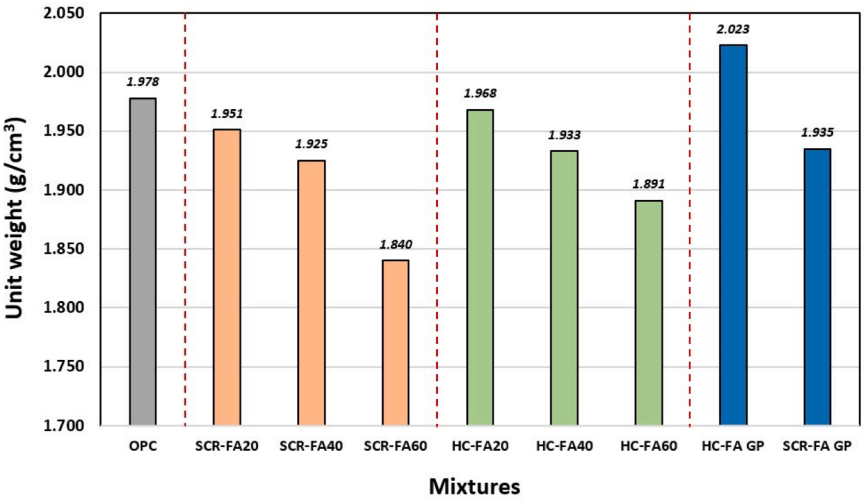

Fig. 8. Dry unit weight of cement pastes at 28-days age.

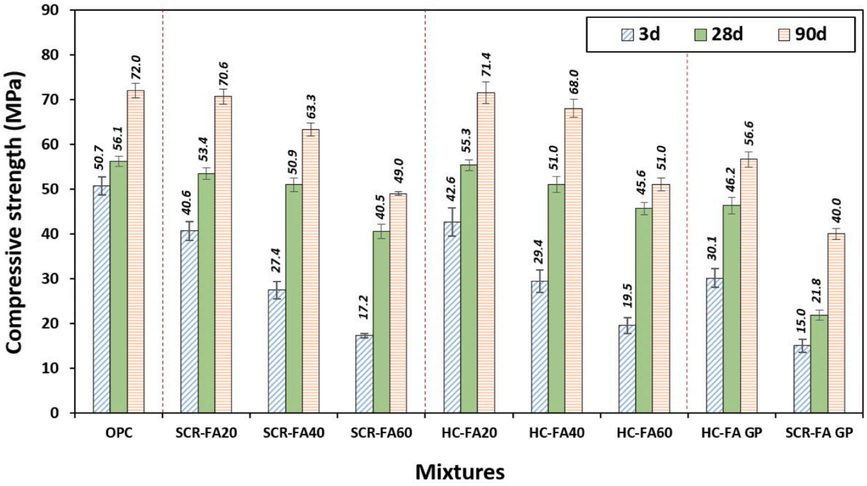

Fig. 9. Compressive strength of all mixtures at 3-, 28- and 90-day age.

$$Ca(OH)_2 + (NH_4)_2SO_4 \rightarrow CaSO_4 \bullet 2H_2O + 2NH_4OH \quad (2)$$

The geopolymer cement pastes exhibited similar strength performance trends to the OPC-fly ash blends. The HC-fly ash geopolymers displayed compressive strength of 30.1 MPa, 46.2 MPa, and 56.6 MPa at 3, 28, and 90 days, respectively. Conversely, the SCR-fly ash geopolymers recorded lower compressive strengths of 15.0 MPa, 21.8 MPa, and 40.0 MPa at the same respective ages. At the standard cement testing age of 28 days, it was found that in geopolymer mixtures, SCR-fly ash (21.8 MPa) exhibits significantly lower compressive strength compared to HC-fly ash (46.2 MPa), with a reduction of approximately 52.8 %.

The difference in strength between OPC-SCR-fly ash blends and SCR-fly ash-based geopolymers is due to their distinct bonding mechanisms and the distribution of reaction products. In OPC-SCR-fly ash systems, C-S-H gel forms through hydration and pozzolanic reactions, ensuring a strong, interwoven microstructure despite ammonia residue, which remains dispersed in the pore solution. This results in only a slight 3.4 % strength reduction. In contrast, geopolymer strength relies on N-A-S-H/C-A-S-H gels formed via alkaline activation, which are highly susceptible to residual ammonium salts. Ammonium sulfate and chloride disrupt geopolymerization by encapsulating fly ash particles, preventing full dissolution, and weakening the gel network. This leads to higher porosity, microcracking, and a drastic 52.8 % strength reduction. SEM and FT-IR analyses confirm that OPC-based samples exhibit a dense, well-formed C-S-H matrix, whereas geopolymer samples contain unreacted fly ash, voids, and disrupted aluminosilicate bonding. Thus, the primary reason for poor geopolymer performance is the destabilizing effect of ammonium salts on gel formation, which weakens the structural integrity compared to the more robust C-S-H network in OPC blends.

Overall, the 20 % replacement of both SCR-fly ash (SCR-FA20) and HC-fly (HC-FA20) exhibited promising results in terms of good early strength (3 days) and later age strength comparable to the reference mix. Blending fly ash with OPC offers several other benefits, including reduced overall cost, lower hydration heat and enhanced workability. At 40 % replacement level, both fly ash types also demonstrated good performance, albeit with lower strength and exceeding the 25 % limit stipulated by ACI 318M-99 [24]. However, the geopolymers systems, in particular those containing SCR fly ash, performed less well compared to the OPC blends. The larger particle size and residual ammonia contamination in SCR fly ash are postulated to be the primary factors behind its lower strength development. These findings emphasize the critical effects of physical and chemical characteristics in the overall performance of cementitious materials [18,26,27].

3.4. Microstructure

Fig. 10 shows examples of SEM micrographs of 28-day OPC-fly ash blended pastes at 20 %, 40 %, and 60 % replacement levels. Qualitatively, the pastes with 20 % SCR-fly ash and 20 % HC-fly ash exhibit a more compact microstructure, which correlates to their enhanced compressive strength, compared to higher fly ash replacement levels (40 % and 60 %). Many unreacted fly ash particles are present with SCR-fly ash being larger in particle size compared to HC-fly. Additionally, the presence of C-S-H, portlandite and ettringite is observed within the microstructure, indicating active hydration processes.

In contrast, the SEM micrographs for pastes containing 40 % and 60 % fly ash reveal higher amounts of unreacted fly ash particles as expected, and increased porosity relative to the 20 % fly ash pastes. This is consistent with their lower compressive strengths. The most pronounced structural weaknesses are seen in the mixtures with 60 % fly ash, which exhibits the most porous microstructure, with numerous microcavities and voids filled with unreacted fly ash particles. This demonstrates that excessive replacement of OPC with fly ash compromises the material integrity.

Fig. 11 presents the SEM micrographs of 28-day geopolymers. The SCR-fly ash geopolymers exhibit a more porous microstructure

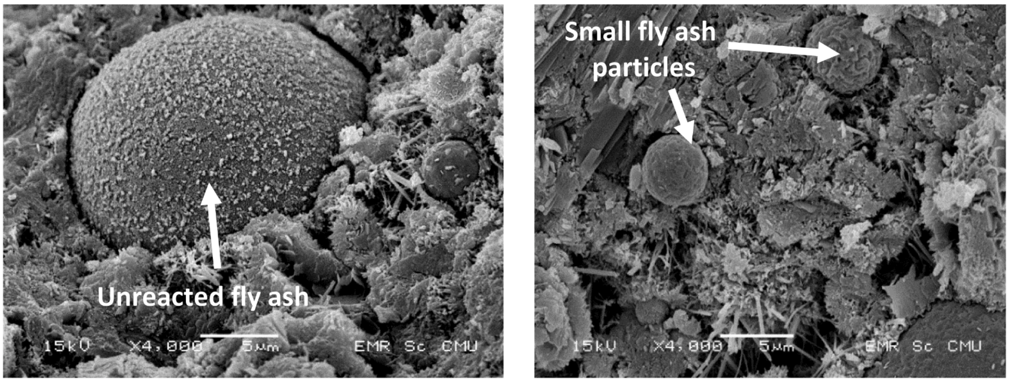

a) SCR-FA20 (left) and HC-FA20 (right)

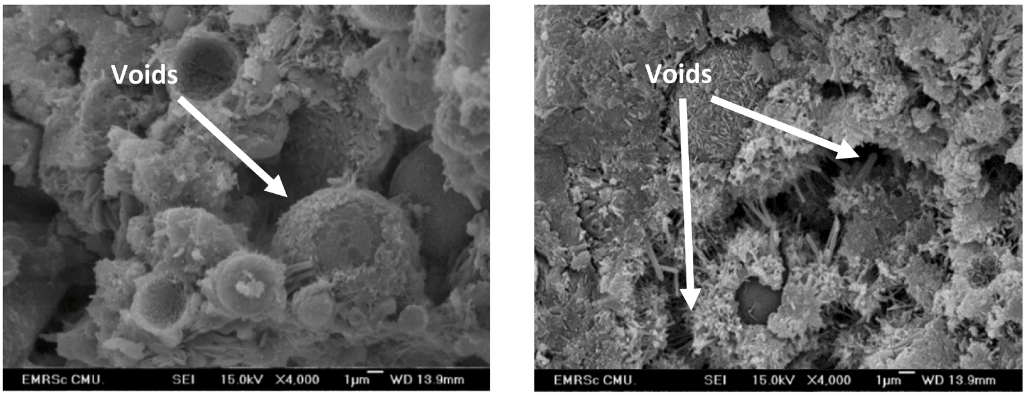

b) SCR-FA40 (left) and HC-FA40 (right)

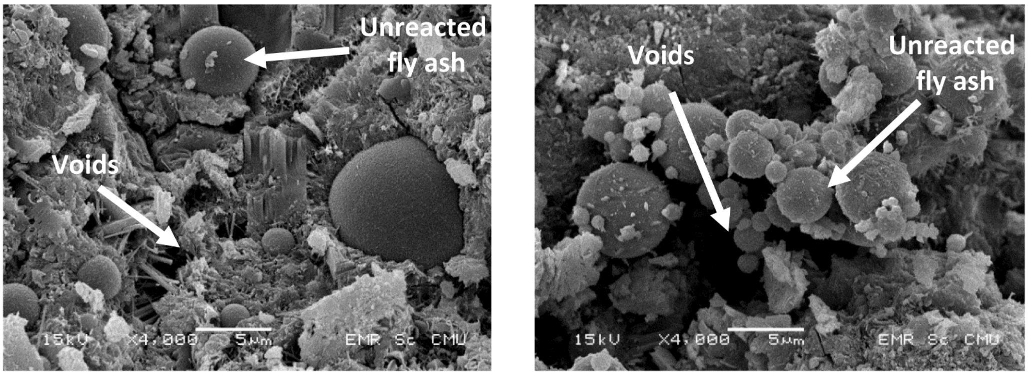

c) SCR-FA60 (left) and HC-FA60 (right)

Fig. 10. Example SEM micrographs of OPC-fly ash pastes at 28 days.

with abundant micro-cracks. In contrast, the HC-fly ash geopolymers are more compact and denser, presumably due to their composition, finer particle size, and higher reactivity. These observations are consistent with the setting time, unit weight and compressive strength data. The SEM micrographs show that fine fly ash particles efficiently dissolve in the alkaline activator and undergo polymerization over time. Although the geopolymers were cured under ambient conditions rather than at elevated temperatures, an extended curing period allows the polymerization process to occur and achieve good compressive strength at later ages, comparable to the OPC-fly ash blended pastes.

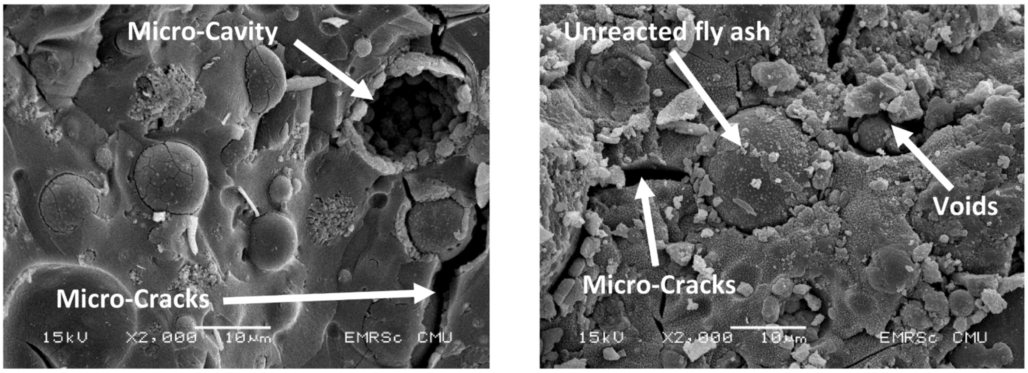

a) SCR-FA GP

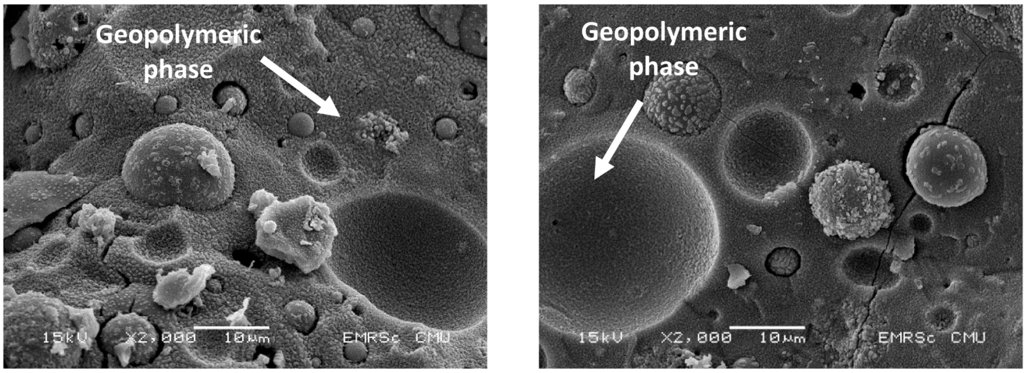

b) HC-FA GP

Fig. 11. Example SEM micrographs of geopolymer cement pastes at 28 days.

3.5. Phase analysis and functional groups

3.5.1. XRD

The XRD patterns of all mixtures at 28-day are presented in Fig. 12. The OPC paste shows the presence of calcium silicate hydrate, calcium hydroxide and calcite, and small amounts of ettringite and mullite. A similar trend was observed in the OPC-fly ash blended pastes. With increasing fly ash content (20 %, 40 %, and 60 %), a broad hump at around 30° 2-theta appears, indicating an increased presence of amorphous phase that forms via the pozzolanic reaction. Additionally, small peaks of quartz were observed, attributed to the silica content in the binders.

Notably, pastes with high amounts of SCR-fly ash (SCR-FA40 and SCR-FA60) exhibited small peaks of gypsum ($CaSO_4$) and ammonium salt (NH_4Cl). These results are supported by the studies of Skaf [29] and Li et al. [28], which indicate that ammonia can react with sulphur oxides, leading to the formation of ammonium sulfate and bisulphate. These compounds can encapsulate fly ash particles, altering their physical characteristics, promoting agglomeration, and resulting in larger particle sizes compared to HC-fly ash. However, only small peaks were observed in this study because the SCR-fly ash used had been stored for over 200 days before testing. Consequently, the XRD detected only a minimal amount of these compounds [28–30].

This is likely due to the trace ammonia remaining in the SCR-fly ash after 200 days of storage prior to casting (Fig. 4). This suggests a longer storage period for SCR-fly ash may not necessarily eliminate the potential for these undesirable phases to form.

Significant differences in XRD patterns were observed in the geopolymer mixtures, which form predominantly amorphous calcium aluminate silicate hydrate (C-A-S-H) and sodium aluminate silicate hydrate (N-A-S-H). Although small peaks of quartz (Q) and calcite (C') were observed, the majority of the phase assemblage is amorphous as indicated by the broad hump at around 30° 2-theta, consistent with the SEM micrographs shown in Fig. 11. Table 3 shows a qualitative assessment of the relative percentages of the crystalline and amorphous phases calculated using the embedded XRD software Match! following Eqs. (3) and (4).

$$\%\mathrm{Amorphous} = \frac{(Global\ area - Reduced\ area)}{Global\ area} * 100 \tag{3}$$

$$\%\mathrm{Crystalline} = 100 - \%\mathrm{Amorphous} \tag{4}$$

Where the global area represents the cumulative sum of areas under both the hump and peaks in the specified region of the XRD

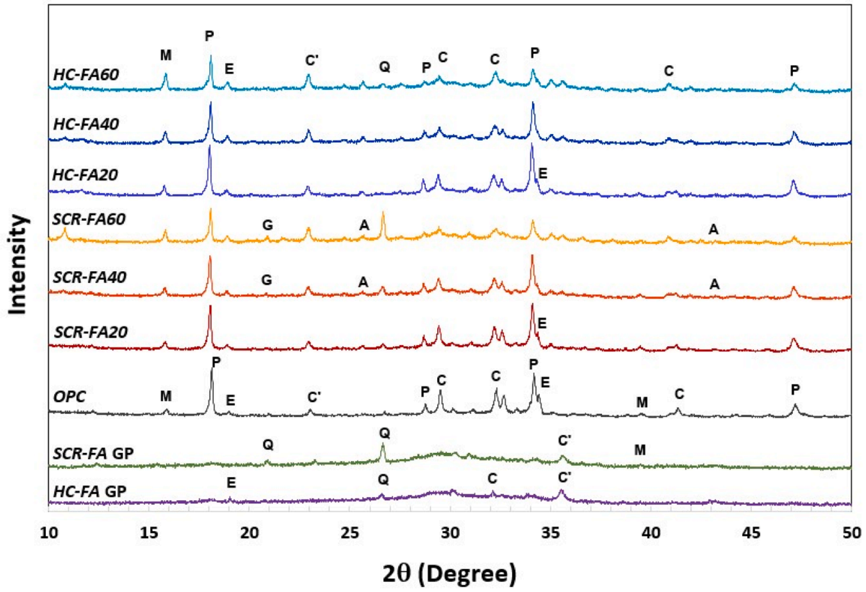

Fig. 12. XRD patterns of OPC and fly ash-based mixtures at 28 days (M = Mullite, C' = Calcite, C = Calcium Silicate Hydrate (C-S-H), E = Ettringite, P = Portlandite ($Ca(OH)_2$), Q = Quartz, G = Calcium sulfate, A = Ammonium salt).

Table 3
Percentages of crystalline and amorphous phases of all mixtures at 28 days.

Mixtures	Global area	Reduced area	% Amorphous	% Crystallinity
OPC	4360.70	2823.74	35.22	64.78
HC-FA60	4674.67	2674.26	42.77	57.23
HC-FA40	4822.42	2851.20	40.86	59.14
HC-FA20	5105.98	3058.71	40.07	59.93
SCR-FA60	4864.50	2762.94	43.19	56.81
SCR-FA40	4713.41	2759.60	41.44	58.56
SCR-FA20	4668.12	2910.05	37.64	62.36
SCR-FA GP	4113.44	971.98	76.37	23.63
HC-FA GP	3952.23	860.01	78.24	21.76

spectrum, while the reduced area represents the sum of areas under the peaks only. The results confirm that geopolymers are predominantly amorphous (> 75 %). In contrast, the phase assemblage of the OPC and OPC-fly ash blended paste are predominantly crystalline, with the percentage of crystallinity decreasing with increasing fly ash replacement level as expected.

3.5.2. FT-IR

Fig. 13 shows the FT-IR spectra of the fly ash and geopolymer mixtures. The broad absorption bands around 3450 cm^{-1} and 1650 cm^{-1} correspond to O-H stretching and bending vibrations, indicating the presence of hydroxyl groups, likely from water or hydroxide ions in the systems. The bands in the range of 1400–1420 cm^{-1} indicate internal reactions of asymmetric Si—O and Al—O bonding in both SCR- and HC-fly ash geopolymers. The presence of ammonia residues, detected at around 1400 cm^{-1}, suggests the formation of ammonium salts, which appear more intense in SCR-FA GP compared to HC-FA GP. These ammonium salts may be ammonium chloride (NH_4Cl) from N-H bending or ammonium sulfate ($(NH_4)_2SO_4$) from N-H stretching vibrations, and they could explain the lower compressive strength of the SCR-fly ash geopolymers.

The Si-O symmetric stretching groups, corresponding to the band around 1110 cm^{-1}, were detected in high-calcium fly ash powder and HC-fly ash geopolymer cement. This indicates the formation of more polymeric Si—O—Si bonds, which contribute to stronger and more interconnected geopolymeric chains within the hardened geopolymer cement at later ages. Additionally, the intensity of the peaks from 950 to 956 cm^{-1} presents the Si-O and Al-O stretching vibrations of SiO_4 and AlO_4, which are indicative of geopolymeric gel and mixed (C,N)-A-S-H gel. The Si-O and Al-O symmetric stretching vibrations in C-S-H appear at the peak of 870 cm^{-1}, indicating the formation of C-(A)-S-H. Overall, the FTIR analysis demonstrates the transformation of fly ash materials to geopolymeric structures, via the development of aluminosilicate networks and hydration products [7,16,17].

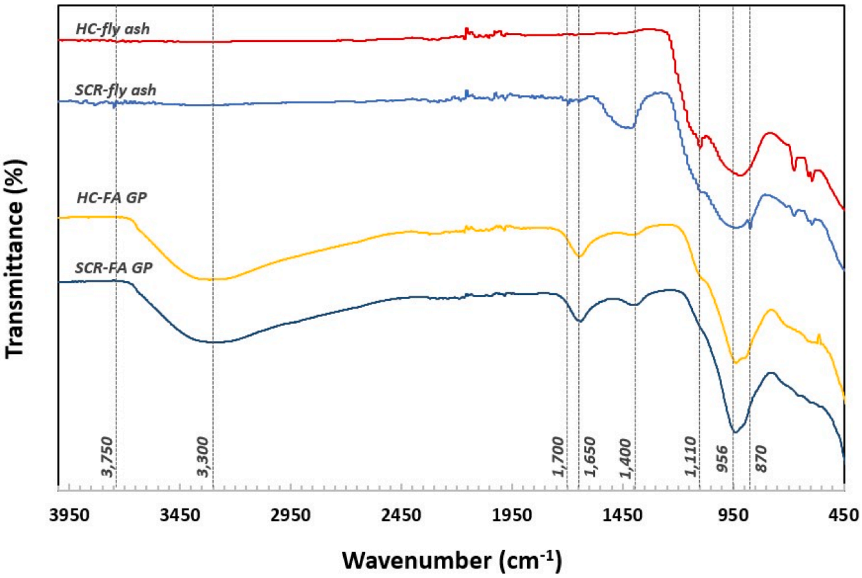

Fig. 13. FT-IR analysis of fly ash and geopolymer mixtures at 28 days.

4. Conclusions

This paper presents an experimental study on the potential of ammonia-contaminated fly ash from the selective catalytic reduction (SCR) process as a viable supplementary cementitious material in OPC blended and geopolymer cement systems. The properties and effects of SCR-fly ash are compared against conventional high-calcium (HC) fly ash. The main findings are:

a) The particle size and surface area of fly ash affect the setting time and flowability of fresh OPC-fly ash blended cement paste. The smaller spherical particles of HC-fly ash increased their reactivity, resulting in a shorter setting time and lower flow value compared to the coarser SCR-fly ash.
b) SCR-fly ash can be used as a supplementary cementitious material to partially replace OPC. At 20 % replacement, SCR-fly ash performs similar to typical HC-fly ash, with only a slight reduction in compressive strength. It offers the advantage of reducing Portland cement consumption while maintaining good engineering properties.
c) However, it is crucial that SCR-fly ash be exposed to the ambient atmosphere for at least 20 days to allow the release of residual ammonia. Excessive ammonia content could lead to the formation of deleterious gypsum or ammonium salt, which affects reactivity and strength development.
d) In conclusion, this new type of fly ash from selective catalytic reduction process at the Mae Moh power plant in Lampang province, Thailand, demonstrates potential as a supplementary cementitious material. However, it may not be suitable as precursor for geopolymer due to its significantly lower mechanical properties compared to HC-fly ash. This study serves as an initial investigation into the potential applications of SCR-fly ash.

CRediT authorship contribution statement

Fan Mizi: Writing – review & editing, Visualization, Validation, Supervision. **Suwan Teewara:** Writing – review & editing, Writing – original draft, Visualization, Validation, Supervision, Resources, Project administration, Methodology, Investigation, Funding acquisition, Formal analysis, Conceptualization. **Jitsangiam Peerapong:** Visualization, Supervision. **Wong Hong:** Writing – review & editing, Visualization, Validation, Supervision, Formal analysis. **Chindaprasirt Prinya:** Visualization, Supervision. **Hansapinyo Chayanon:** Visualization, Supervision.

Declaration of Competing Interest

The authors declare that they have no known competing financial interests or personal relationships that could have appeared to influence the work reported in this paper

Acknowledgements

This research work was supported by Fundamental Fund 2025, Chiang Mai University. The authors would like to express their gratitude to the Department of Civil Engineering, Faculty of Engineering, Chiang Mai University, for providing the necessary equipment and facilities. Special thanks are due to Mr. Teerapad Jongwijak (M.Eng) for his dedicated efforts on this project. Thanks to the Electricity Generating Authority of Thailand (EGAT 68-N402000-11-IO.SS03N3008692) for their kind support. The authors also wish to acknowledge the cooperation and support from Brunel University, Imperial College London and Khon Kaen University.

Data availability

Data will be made available on request.

References

[1] S. Gupta, S. Chaudhary, Use of fly ash for the development of sustainable construction materials, in: New Materials in Civil Engineering, Butterworth-Heinemann, 2020, pp. 677–689.
[2] A.R. Gollakota, V. Volli, C.M. Shu, Progressive utilisation prospects of coal fly ash: a review, Sci. Total Environ. 672 (2019) 951–989.
[3] ASTM International, ASTM C618: Standard Specification for Coal Fly Ash and Raw or Calcined Natural Pozzolan for Use in Concrete, ASTM International, 2023.
[4] P.R. De Matos, M. Foiato, L.R. Prudêncio Jr, Ecological, fresh state and long-term mechanical properties of high-volume fly ash high-performance self-compacting concrete, Constr. Build. Mater. 203 (2019) 282–293.
[5] P. Jitsangiam, T. Suwan, K. Pimraksa, P. Sukontasukkul, P. Chindaprasirt, Challenge of adopting relatively low strength and self-cured geopolymer for road construction application: a review and primary laboratory study, Int. J. Pavement Eng. 22 (11) (2021) 1454–1468.
[6] P. Cong, Y. Cheng, Advances in geopolymer materials: a comprehensive review, J. Traffic Transp. Eng. (Engl. Ed.) 8 (3) (2021) 283–314.
[7] T. Suwan, M. Fan, N. Braimah, Micro-mechanisms and compressive strength of geopolymer-Portland cementitious system under various curing temperatures, Mater. Chem. Phys. 180 (2016) 219–225.
[8] C. Lu, D. Wang, W. Zhu, F. Wang, Z. Du, Y. Zhu, Performance evaluation and life management of SCR denitration catalyst, IOP Conf. Ser.: Earth Environ. Sci. 495 (1) (2020) 012035.
[9] A. Michalik, J. Babińska, F. Chyliński, A. Piekarczuk, Ammonia in fly ashes from flue gas denitrification process and its impact on the properties of cement composites, Buildings 9 (11) (2019) 225.
[10] E.N. Nedkvitne, Ammonia Hydrometallurgy and Other Innovations for Sustainable Management of Waste Incineration Fly Ash, 2024.
[11] L. Larrimore, Effects of ammonia from post-combustion NOx control on ash handling and use, Fuel Chem. Div. Prepr. 47 (2) (2002) 832–833.
[12] European Environment Agency, Directive 2010/75/EU of the European Parliament and of the Council of 24 November 2010 on industrial emissions (integrated pollution prevention and control), 2010. Available at: ⟨https://www.eea.europa.eu/policy-documents/directive-2010-75-eu-of⟩ (Accessed 11 January 2024).
[13] T.S. Yelland. Cleaner Coal Combustion Technologies–The Impact on NOx Emissions and Fireside Corrosion (Doctoral dissertation), University of Sheffield, 2020.
[14] O. Kröcher, Selective catalytic reduction of NOx, Catalysts 8 (10) (2018) 459.
[15] G.F. Brendel, J.E. Bonetti, R.F. Rathbone, R.N. Frey Jr, Investigation of Ammonia Adsorption on Fly Ash Due to Installation of Selective Catalytic Reduction Systems, West Virginia University Research Corporation, US, 2000.
[16] M. Xu, Y. Wu, P. Zhang, Z. Liu, Z. Hu, Q. Lu, Green and moderate activation of coal fly ash and its application in selective catalytic reduction of NO with NH3, Environ. Sci. Technol. 56 (4) (2022) 2582–2592.
[17] F. Chyliński, A. Goljan, A. Michalik, Fly ash with ammonia: properties and emission of ammonia from cement composites, Materials 14 (4) (2021) 707.
[18] Y. Zhao, H. Luan, B. Yang, Z. Li, M. Song, B. Li, X. Tang, Adsorption of low-concentration ammonia nitrogen from water on alkali-modified coal fly ash: characterization and mechanism, Water 15 (5) (2023) 956.
[19] T. Suwan, T. Jongwijak, P. Jitsangiam, C. Buachart, B. Charatpangoon, K. Jitpairod, Utilization of new fly ash type from selective catalytic reduction (SCR) process as an additive in Portland cement. International Conference on Environment Sciences and Renewable Energy, Springer Nature Singapore, Singapore, 2022, pp. 125–134.
[20] P. Zhang, W. Yu, B. Gao, S. Cui, J. Li, L. Qi, Denitration performance and mechanism of Mn-Ce supported alkali-modified fly ash catalysts for NH3-SCR, Fuel 357 (2024) 129878.
[21] A. Al-Otaibi, Barriers and enablers for green concrete adoption: a scientometric aided literature review approach, Sustainability 16 (12) (2024) 5093.
[22] M. Elzeadani, D.V. Bompa, A.Y. Elghazouli, One-part alkali-activated materials: a state-of-the-art review, J. Build. Eng. 57 (2022) 104871.
[23] L.N. Assi, E.E. Deaver, P. Ziehl, Effect of source and particle size distribution on the mechanical and microstructural properties of fly ash-based geopolymer concrete, Constr. Build. Mater. 167 (2018) 372–380.
[24] ACI COMMITTEE 318, Building code requirements for structural concrete (ACI 318M-19) and commentary (ACI 318RM-19), 2022.
[25] T. Suwan, P. Jitsangiam, P. Chindaprasirt, Influence of nano-silica dosage on properties of cement paste incorporating high calcium fly ash, in: Key Engineering Materials, 841, Trans Tech Publications Ltd, 2020, pp. 9–13.
[26] M. Muthu, Ł. Sadowski, Performance of permeable concrete mixes based on cement and geopolymer in aggressive aqueous environments, J. Build. Eng. 76 (2023) 107143.
[27] S.E. Kelechi, M. Adamu, O.A.U. Uche, I.P. Okokpujie, Y.E. Ibrahim, I.I. Obianyo, A comprehensive review on coal fly ash and its application in the construction industry, Cogent Eng. 9 (1) (2022) 2114201.
[28] J. Li, S. Li, M. Zhang, Z. Wang, Y. Shu, J. Liu, X. Huang, Preparation, characterization, and scattering characteristics of mixed aerosol of fly ash and ammonium sulfate, Processes 12 (4) (2024) 769.
[29] Z. Skaf, T. Aliyev, L. Shead, T. Steffen, The state of the art in selective catalytic reduction control, 2014.
[30] W. Farthing, S. Hinton, R.F. Heaphy. Identification of (and Response to) Potential Effects of SCR Technology on Unintended Emissions and Deposits, U.S. Environmental Protection Agency, 2002.